

Supporting Information for

Reviving BVDT-TTF and EVT-TTF salts

Federica Solano,¹ Pascale Auban-Senzier,² Bolesław Barszcz³, Arkadiusz Frąckowiak³, Iwona Olejniczak³, Pere Alemany,⁴ Enric Canadell,^{*,5} Nicolas Zigon^{*,1}, Narcis Avarvari^{*,1}

¹ Univ Angers, CNRS, MOLTECH-ANJOU, SFR MATRIX, F-49000 Angers, France. E-mail: narcis.avarvari@univ-angers.fr; nicolas.zigon@univ-angers.fr

² Université Paris-Saclay, CNRS, UMR 8502, Laboratoire de Physique des Solides, 91405 Orsay, France

³ Institute of Molecular Physics, Polish Academy of Sciences, Smoluchowskiego 17, 60-179 Poznań, Poland

⁴ Departament de Ciència de Materials i Química Física and Institut de Química Teòrica i Computacional (IQTCUB), Universitat de Barcelona, Martí i Franquès 1, 08028 Barcelona, Spain

⁵ Institut de Ciència de Materials de Barcelona, ICMA-B-CSIC, Campus de la UAB, 08193 Bellaterra, Spain, and Royal Academy of Sciences and Arts of Barcelona, Chemistry Section, La Rambla 115, 08002 Barcelona, Spain. E-mail: canadell@icmab.es

SUMMARY

Table S1. Crystallographic data, details of data collection and structure refinement parameters.

Table S2. Stoichiometry and conductivity of BVDT-TTF, EVT-TTF and BEDT-TTF salts.

Figure S1. Temperature dependent resistivity measurement on single crystal for **(BVDT-TTF)_{2.5}(I₃)**.

Figure S2. Temperature dependent resistivity measurement on single crystal for **(BVDT-TTF)₂(ReO₄)**.

Figure S3. Temperature dependent resistivity measurement on single crystal for **(EVT-TTF)(ClO₄)**.

Figure S4. Raman spectrum of **(BVDT-TTF)_{2.5}(I₃)** measured at room temperature with the 632.8 nm excitation line, in the frequency range of the polyiodide stretching vibrations.

Figure S5. ¹H NMR (300 MHz, CDCl₃) of compound **3**.

Figure S6. ¹³C NMR (76 MHz, CDCl₃) of compound **3**.

Figure S7. ¹H NMR (300 MHz, CDCl₃) of compound **4**.

Figure S8. ¹³C NMR (76 MHz, CDCl₃) of compound **4**.

Figure S9. ¹H NMR (300 MHz, CDCl₃) of compound **BVDT-TTF**.

Figure S10. ¹H NMR (300 MHz, CDCl₃) of compound **EVT-TTF**.

Figure S11. ¹³C NMR (126 MHz, DMSO-d₆) of compound **EVT-TTF**.

Figure S12. MS (MALDI-TOF) of compound **BVDT-TTF**.

Figure S13. MS (MALDI-TOF) of compound **4**.

Figure S14. MS (MALDI-TOF) of compound **EVT-TTF**.

Figure S15. MS (MALDI-TOF) of compound **3**.

Table S1 Crystallographic data, details of data collection and structure refinement parameters.

	(BVDI-TTF)(TaF ₆)	(BVDI-TTF) _{2.5} (I ₃)	(BVDI-TTF) ₂ (ReO ₄)	(EVI-TTF)(ClO ₄)
Formula sum	C ₁₀ H ₄ S ₈ , TaF ₆	C ₁₀ H ₄ S ₈ , I _{1.2}	C ₁₀ H ₄ S ₈ , (ClO ₄) _{0.5}	C ₁₀ H ₆ S ₈ , (CH ₂ Cl ₂) _{0.5} , ClO ₄
Formula weight	675.56	532.89	505.71	524.54
Crystal system	orthorhombic	orthorhombic	monoclinic	monoclinic
Space group	<i>Pnmm</i>	<i>Pnma</i>	<i>C2/m</i>	<i>P2₁/c</i>
<i>a</i> /Å	4.8259(3)	3.777(19)	33.133(3)	8.0005(4)
<i>b</i> /Å	17.8935(9)	12.18(14)	12.1739(14)	23.8718(10)
<i>c</i> /Å	10.1805(5)	33.1(9)	3.8263(6)	9.8100(5)
<i>α</i> /°	90	90	90	90
<i>β</i> /°	90	90	93.360(11)	100.649(5)
<i>γ</i> /°	90	90	90	90
<i>V</i> /Å ³	879.11(8)	1523(46)	1540.7(3)	1841.31(16)
<i>Z</i>	2	4	4	4
<i>D_c</i> /g cm ⁻³	2.552	2.324	2.180	1.892
<i>T</i> /K	200	200	200	297
<i>μ</i> /mm ⁻¹	20.964	29.814	18.139	11.819
Reflections collected	883	1518	1714	6003
Independent reflection	826	1207	1035	2614
final <i>R</i> ₁ ^a , <i>wR</i> ₂ ^b [<i>I</i> > 2σ(<i>I</i>)]	0.0393/0.1129	0.0795/0.2430	0.1192/0.3454	0.0570/0.1564
<i>R</i> ₁ ^a , <i>wR</i> ₂ ^b (all data)	0.0408/0.1141	0.0943/0.2540	0.1249/0.3489	0.0646/0.1653
goodness-of-fit on <i>F</i> ²	1.099	1.131	1.097	1.055
Δρ _{min} /Δρ _{max} (e Å ⁻³)	-1.305/2.169	-0.755/1.261	-0.971/1.102	-0.938/0.984
Completeness (%)	99.2	98.4	81.0	94.1
CCDC number	2296888-	2296889-	2296890-	2296891-

$$^a R_1 = \sum ||F_o| - |F_c|| / \sum |F_o|. \quad ^b wR_2 = [\sum w(F_o^2 - F_c^2)^2 / \sum w(F_o^2)^2]^{1/2}; \quad w = 1/[\sigma^2(F_o^2) + (aP)^2 + bP] \quad \text{where } P = [\max(F_o^2, 0) + 2F_c^2]/3.$$

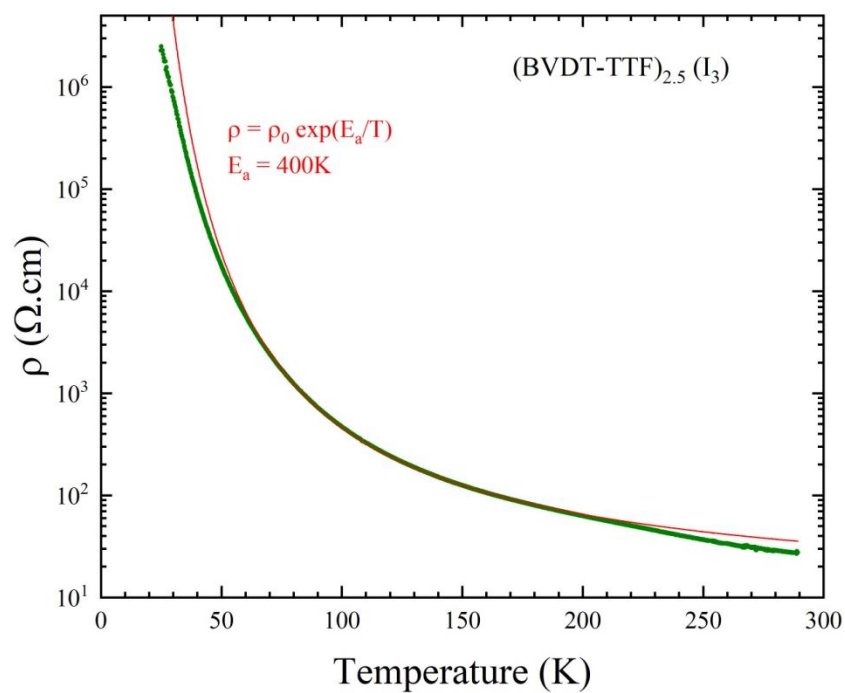


Fig. S1 Temperature dependent resistivity measurement on single crystal for **(BVDT-TTF)_{2.5}(I₃)**.

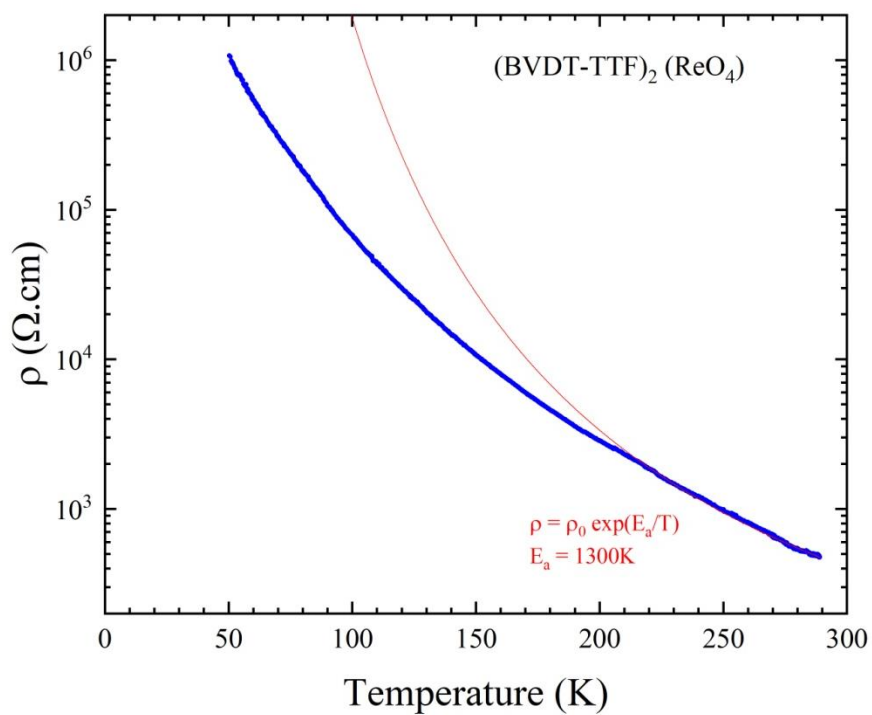


Fig. S2 Temperature dependent resistivity measurement on single crystal for **(BVDT-TTF)₂(ReO₄)**.

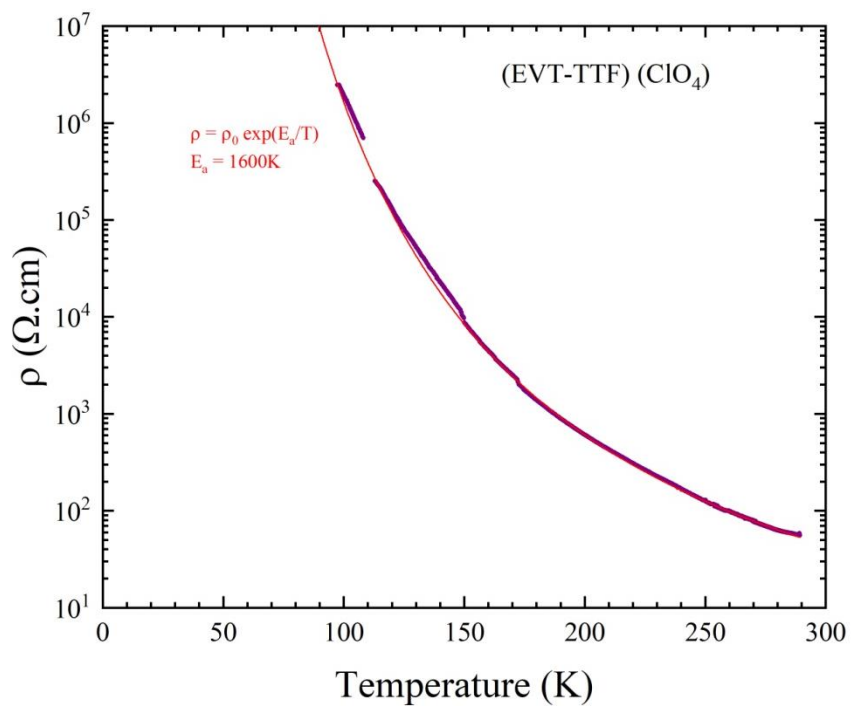


Fig. S3 Temperature dependent resistivity measurement on single crystal for (EVT-TTF)(ClO₄).

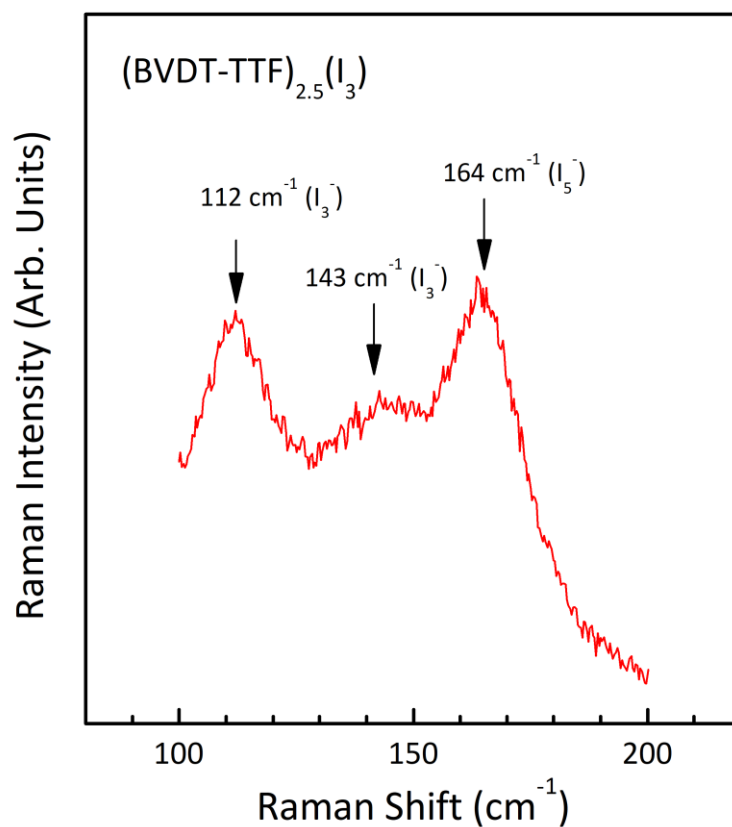


Fig. S4 Raman spectrum of $(\text{BVDT-TTF})_{2.5}(\text{I}_3)$ measured at room temperature with the 632.8 nm excitation line, in the frequency range of the polyiodide stretching vibrations.

The Raman spectrum of $(\text{BVDT-TTF})_{2.5}(\text{I}_3)$ in the frequency range of the stretching polyiodide modes reveals three distinct modes:

- the symmetric stretching of the centrosymmetric triiodide anion at 112 cm^{-1} ,
- the asymmetric stretching mode of the asymmetric triiodide ion at 143 cm^{-1} ,
- the band at 164 cm^{-1} , which is most likely related to the symmetric stretching of the L-shaped pentaiodide present in the structure.^{1,2}

Table S2 Stoichiometry and conductivity of BVDT-TTF, EVT-TTF and BEDT-TTF salts.

Donor	Anion	Stoichiometry	Single crystal conductivity ($\text{S}\cdot\text{cm}^{-1}$, 290K)
BVDT-TTF	TaF_6^-	1 : 1	$4.4\cdot 10^{-2}$
BVDT-TTF	I_3^-	2.5 : 1	$1.4\cdot 10^{-1}$
BVDT-TTF	ReO_4^-	2 : 1	$3.1\cdot 10^{-3}$
EVT-TTF	ClO_4^-	1 : 1	$1.8\cdot 10^{-2}$
BEDT-TTF ³	TaF_6^-	1 : 1	$5\cdot 10^{-4}$
β -BEDT-TTF ⁴	I_3^-	2 : 1	20
BEDT-TTF ⁵	ReO_4^-	2 : 1	$5\cdot 10^{-3}$
BEDT-TTF ⁶	ClO_4^-	2 : 1	26.31

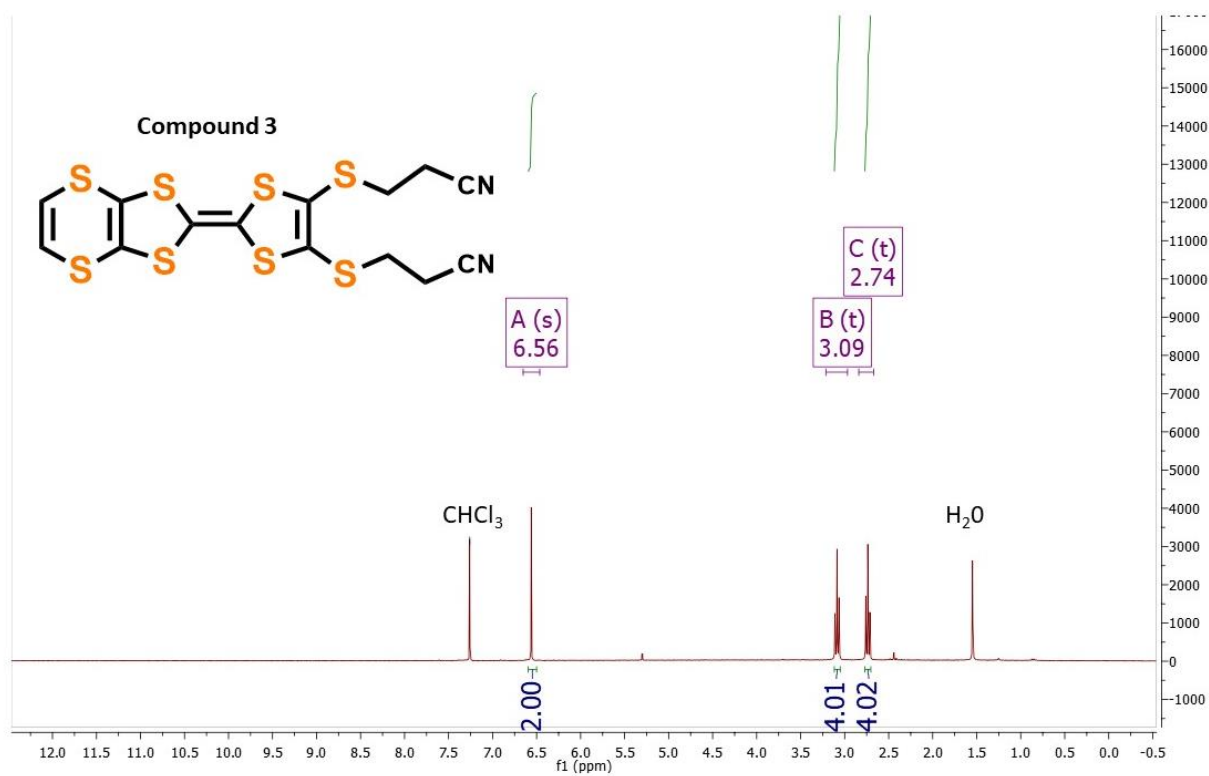


Fig. S5 ¹H NMR (300 MHz, CDCl₃) of compound 3.

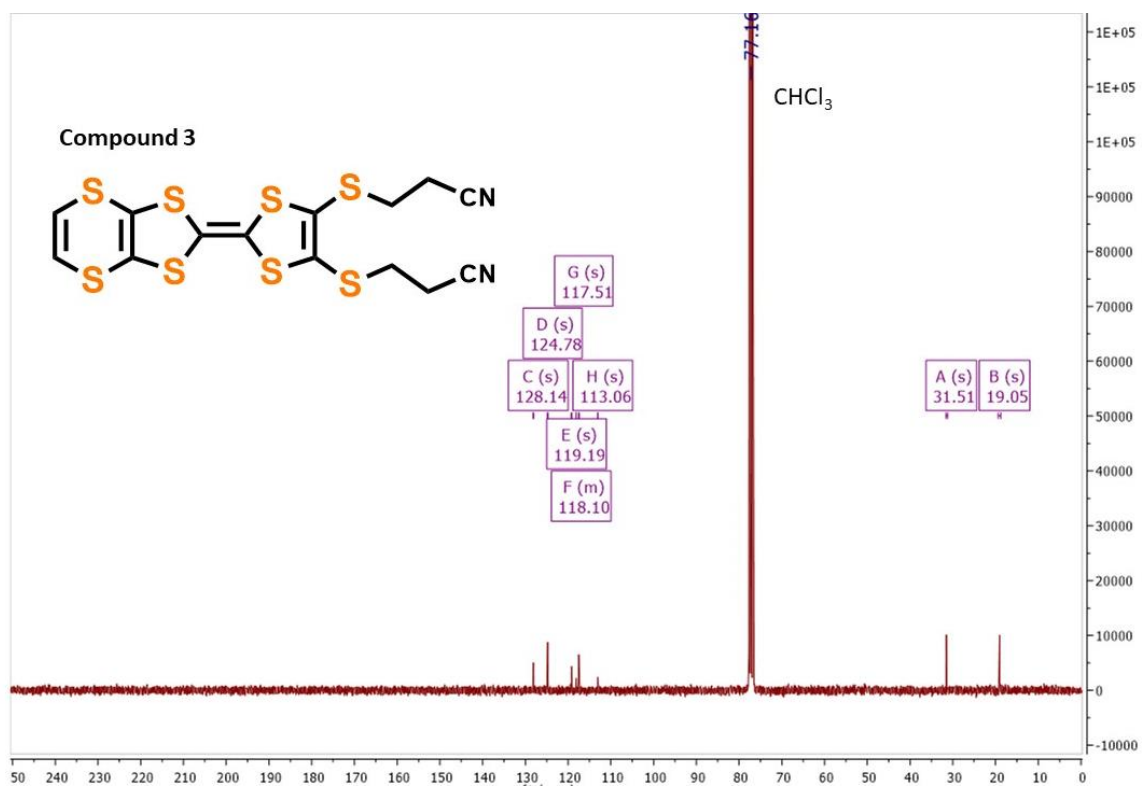


Fig. S6 ¹³C NMR (76 MHz, CDCl₃) of compound 3.

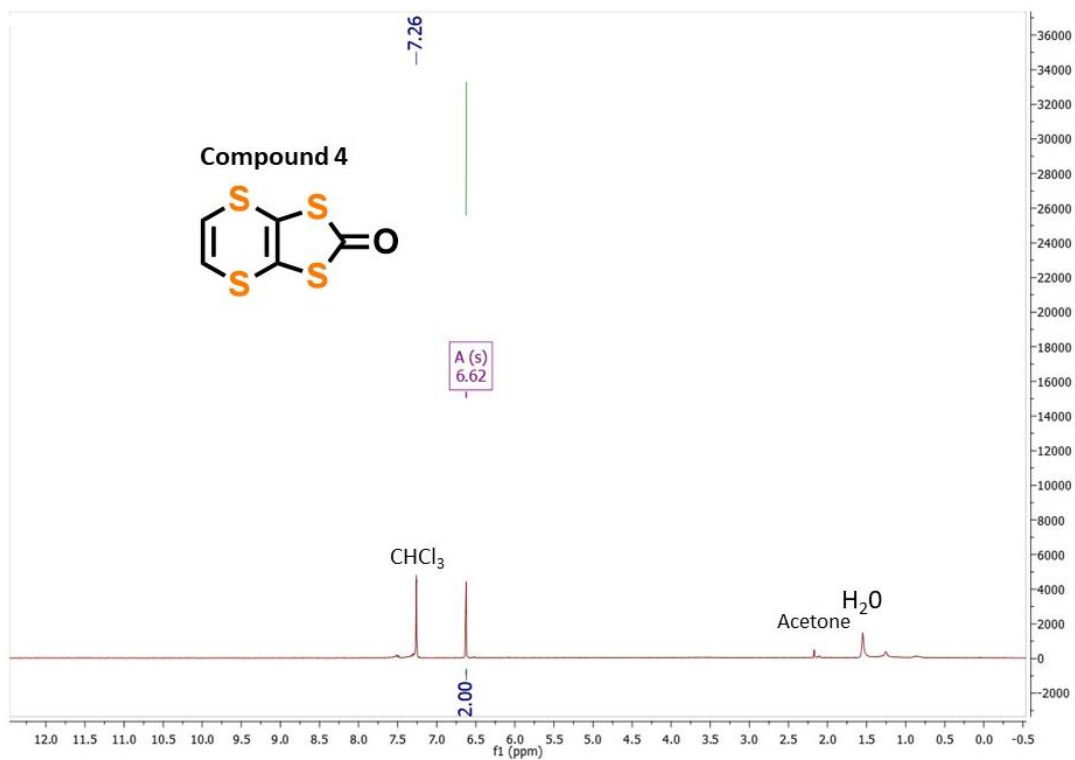


Fig. S7 ¹H NMR (300 MHz, CDCl₃) of compound 4.

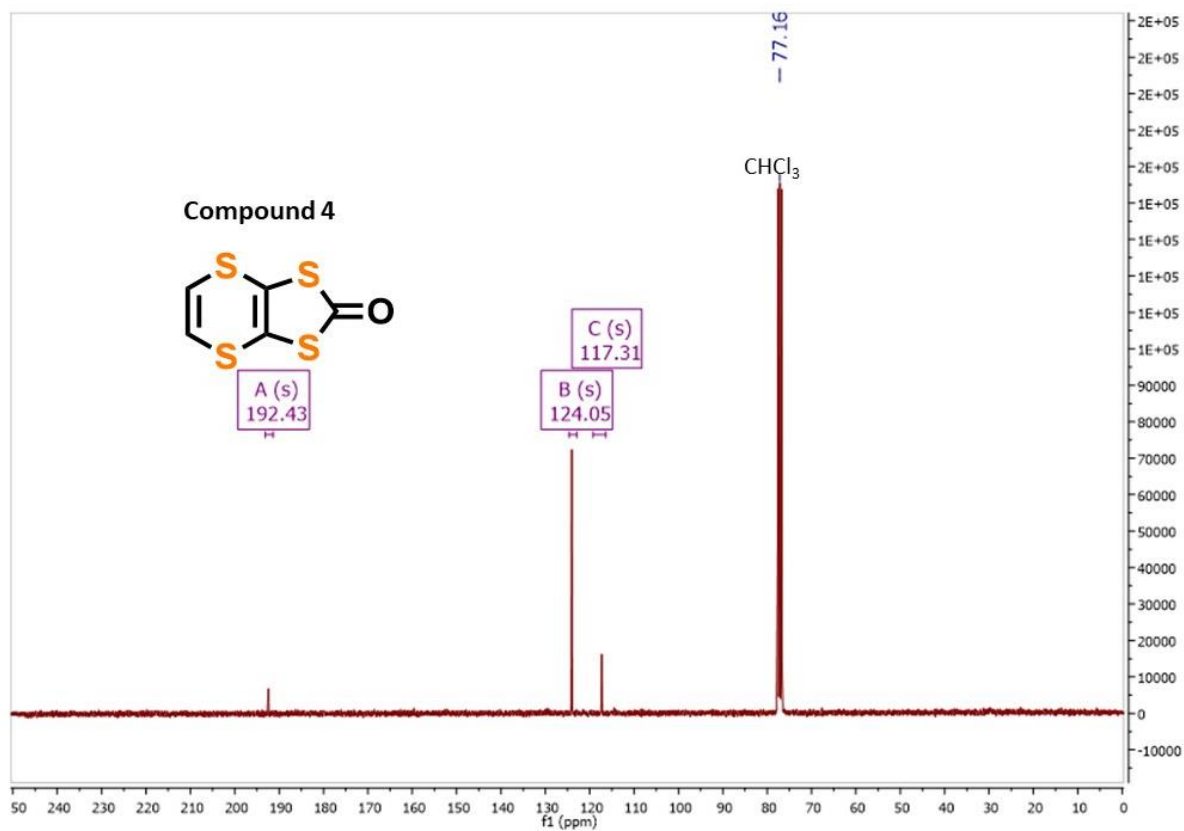


Fig. S8 ¹³C NMR (76 MHz, CDCl₃) of compound 4.

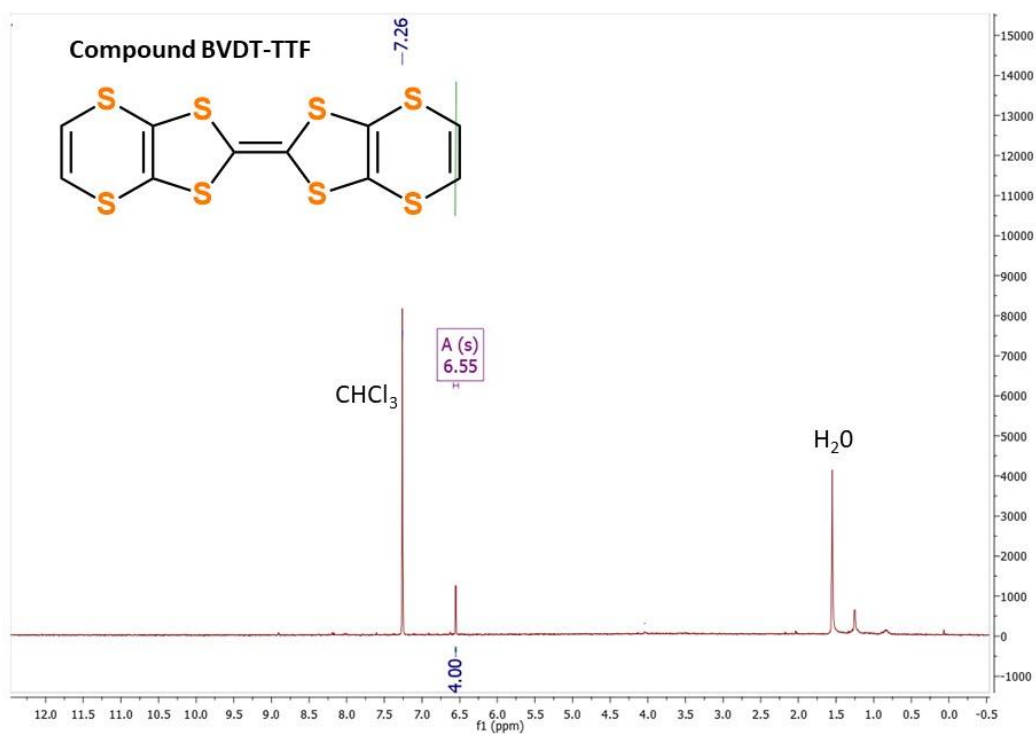


Fig. S9 $^1\text{H NMR}$ (300 MHz, CDCl_3) of **BVD-TTF**.

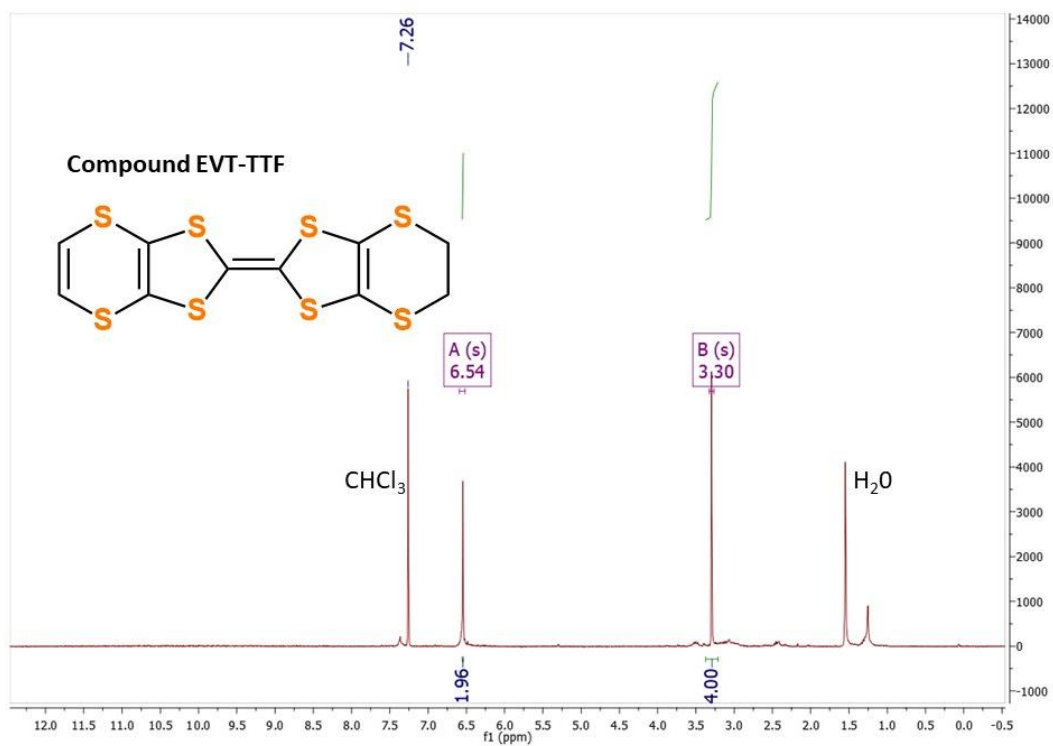


Fig. S10 $^1\text{H NMR}$ (300 MHz, CDCl_3) of **EVT-TTF**.

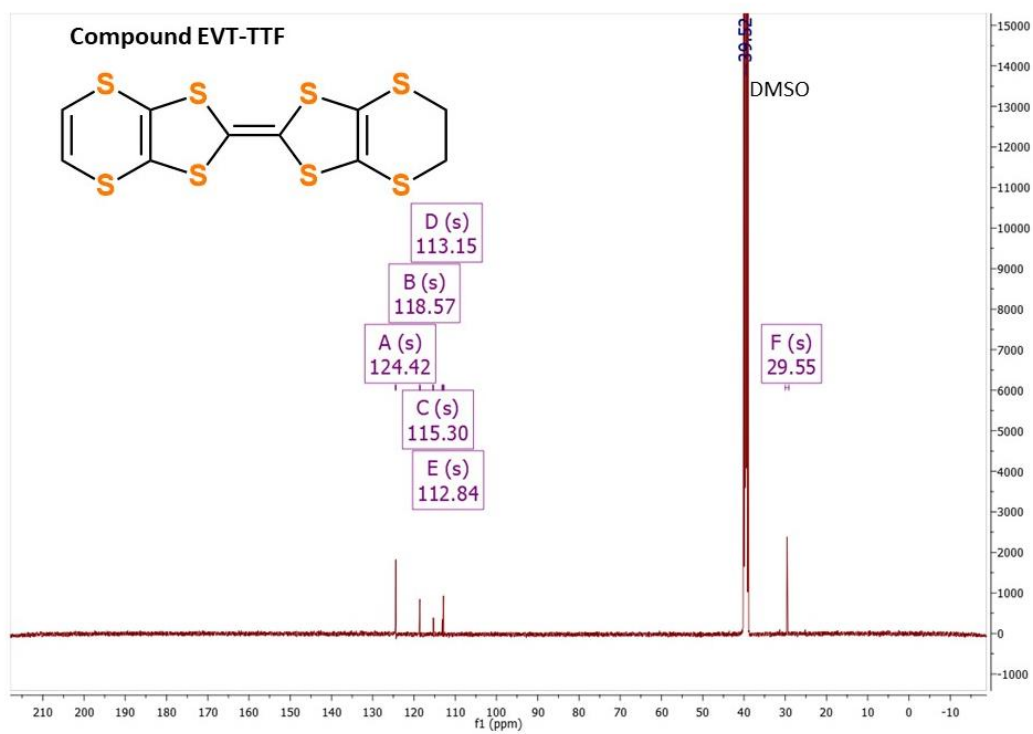


Fig. S11 ^{13}C NMR (126 MHz, DMSO-d_6) of EVT-TTF.

Mass spectrum:

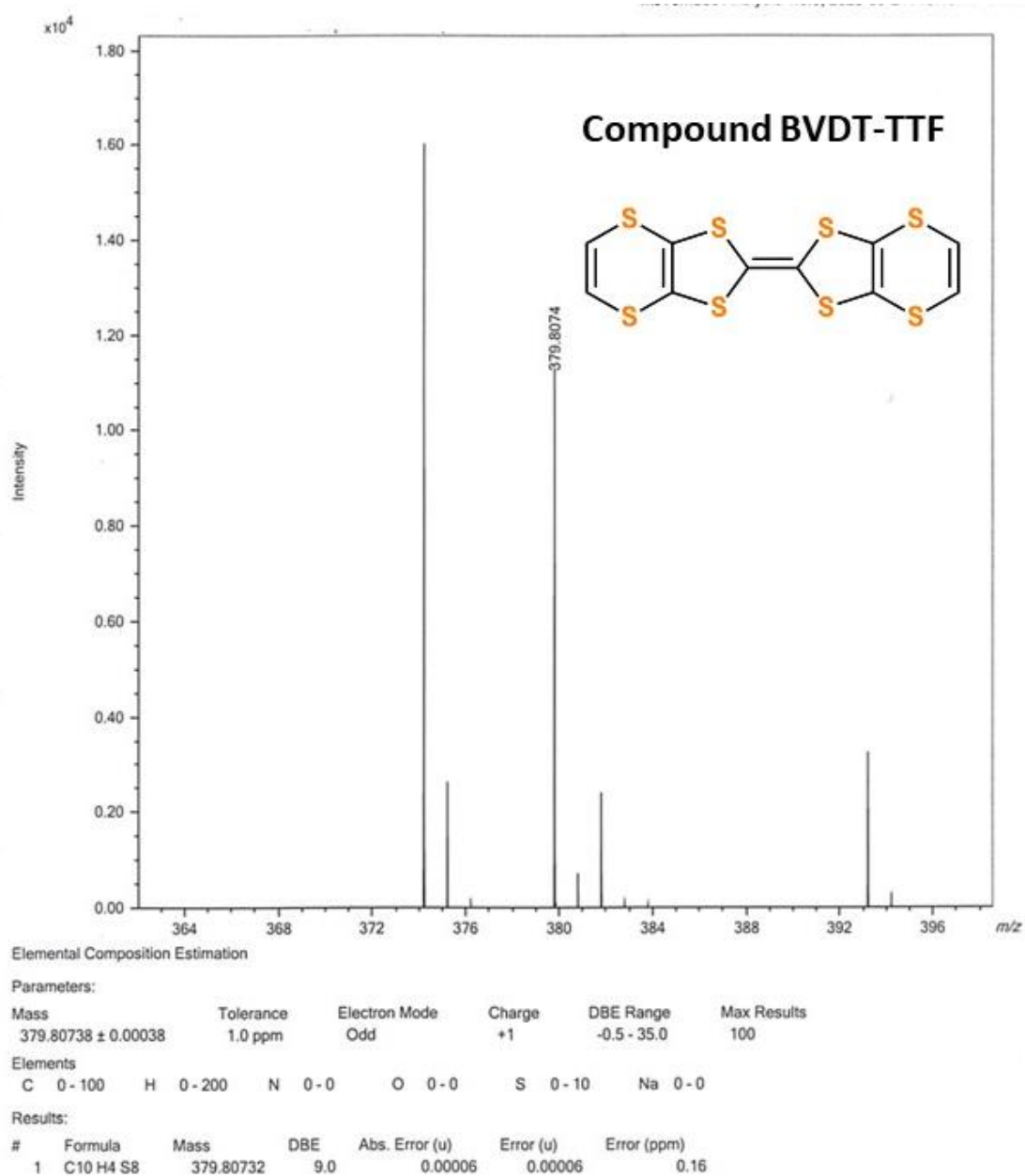


Fig. S12 MS (MALDI-TOF) of BVDT-TTF.

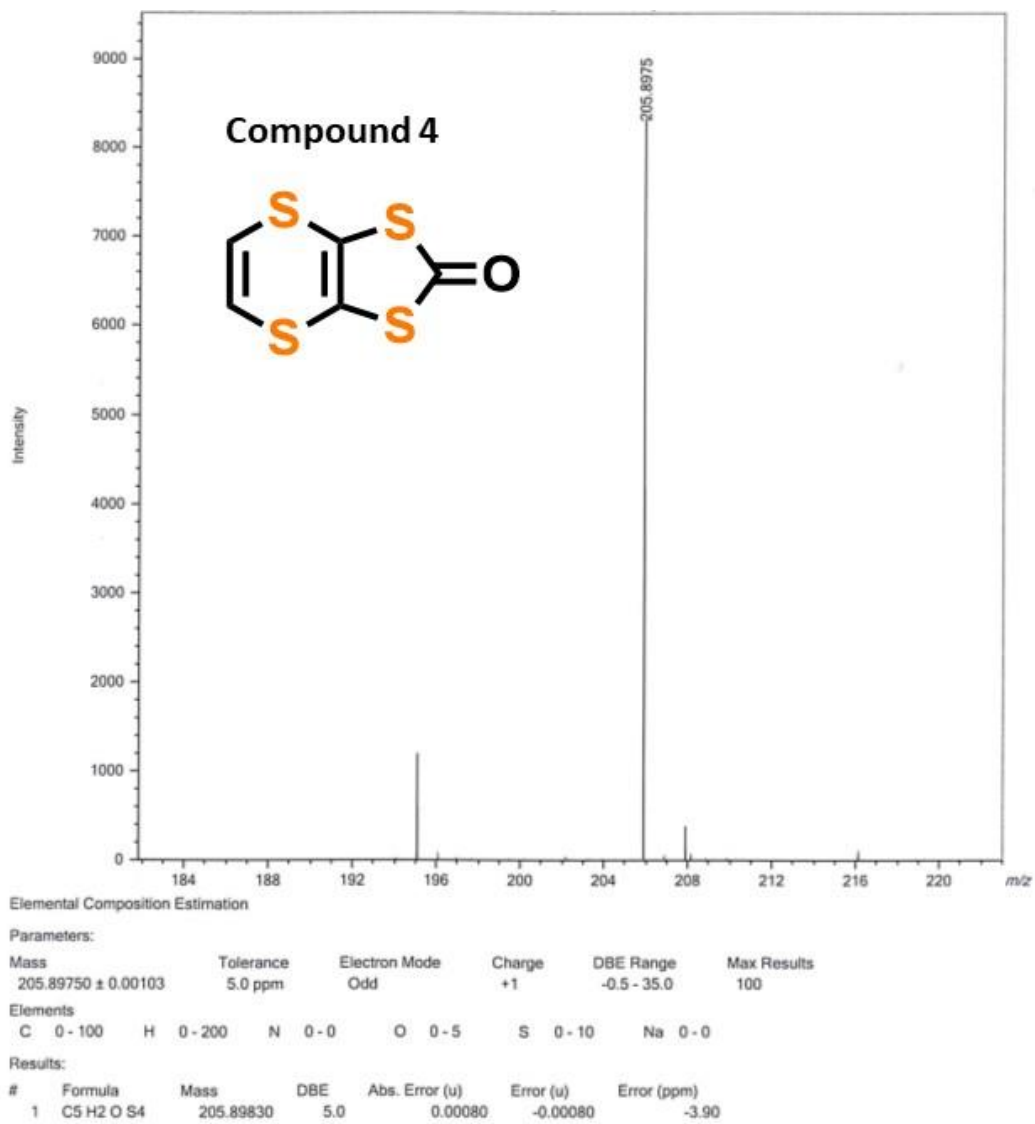


Fig. S13 MS (MALDI-TOF) of compound **4**.

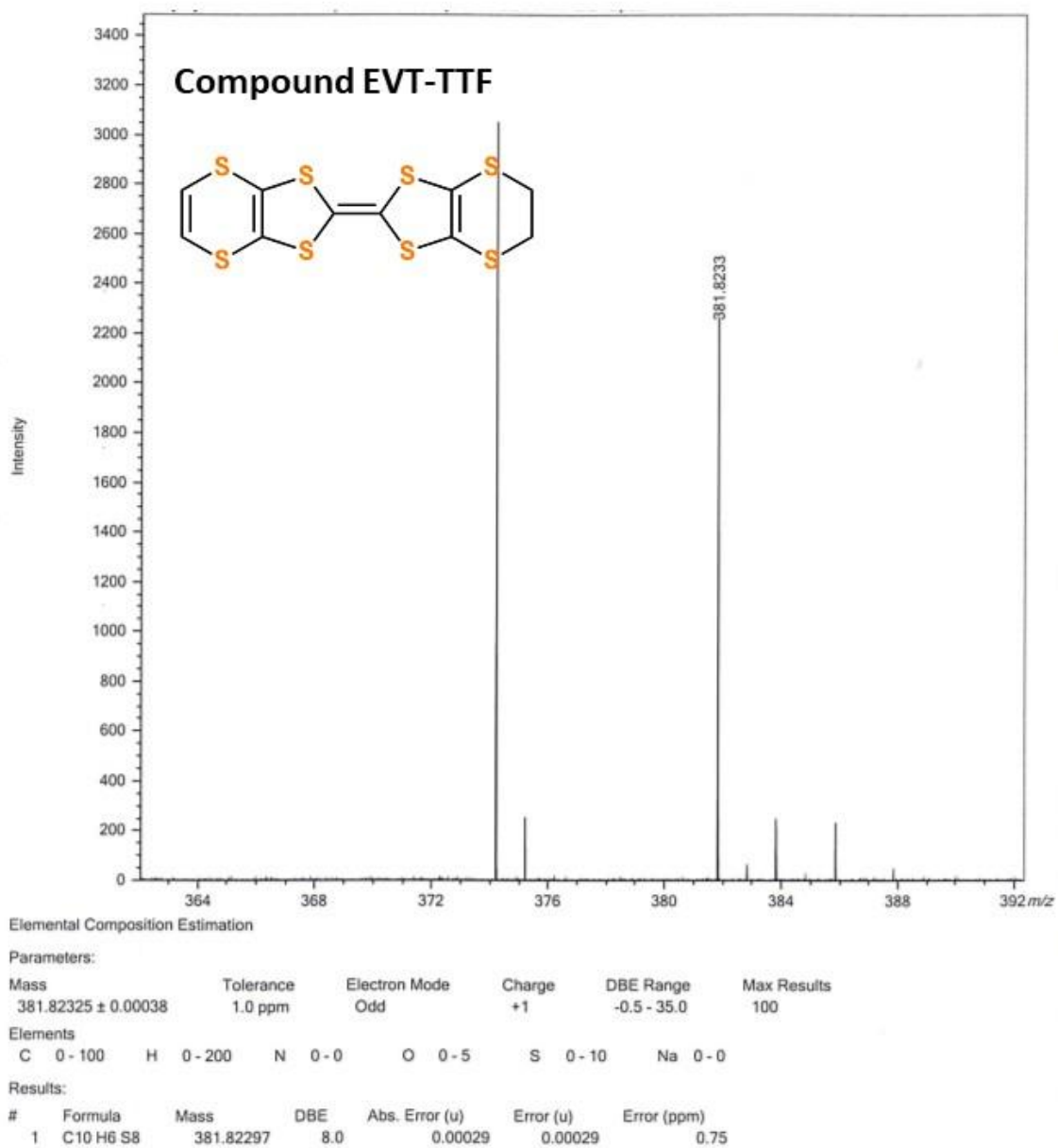


Fig. S14 MS (MALDI-TOF) of EVT-TTF.

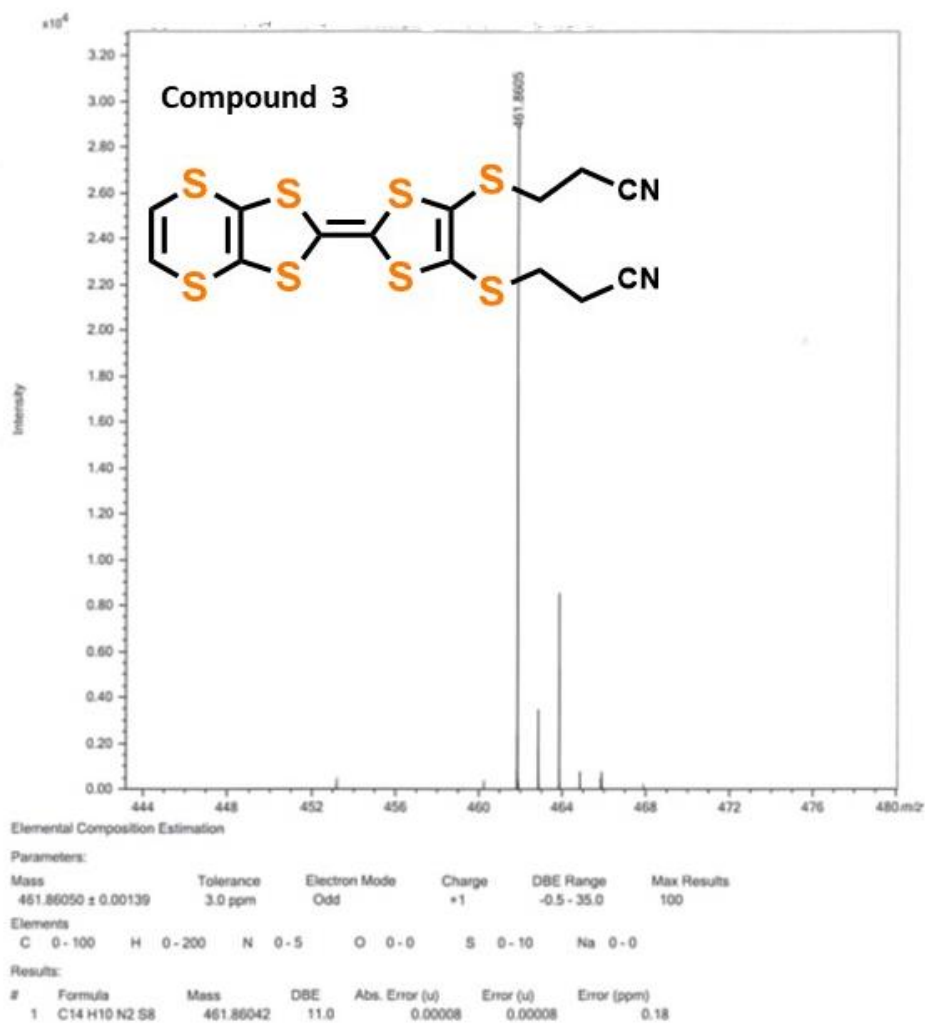


Fig. S15 MS (MALDI-TOF) of compound **3**.

References

- 1 P. H. Svensson and L. Kloo, *Chem. Rev.*, 2003, **103**, 1649–1684.
- 2 I. Jerman, V. Jovanovski, A. Šurca Vuk, S. B. Hočevnar, M. Gaberšček, A. Jesih and B. Orel, *Electrochim Acta*, 2008, **53**, 2281–2288.
- 3 M. Allain, C. Mézière, P. Auban-Senzier and N. Avarvari, *Crystals*, 2021, **11**, 386.
- 4 L. I. Buravov, M. V. Kartsovnik, V. F. Kaminskii, P. A. Kononovich, E. E. Kostuchenko, V. N. Laukhin, M. K. Makova, S. I. Pesotskii, V. N. Topnikov and E. B. Yagubskii, .
- 5 S. S. P. Parkin, E. M. Engler, R. R. Schumaker, R. Lagier, V. Y. Lee, J. C. Scott and R. L. Greene, *Phys. Rev. Lett.*, 1983, **50**, 270–273.
- 6 G. Saito, T. Enoki, K. Toriumi and H. Inokuchi, *Solid State Commun.*, 1982, **42**, 557–560.